frontiers in Earth Science

ORIGINAL RESEARCH
published: 12 January 2021
doi: 10.3389/feart.2020.592659

Magnetic Properties of Plant Ashes and Their Influence on Magnetic Signatures of Fire in Soils

Jessica L. Till[1,2]*, *Bruce Moskowitz*[2] *and Simon W. Poulton*[3]

[1]Institute of Earth Sciences and Institute of Life and Environmental Sciences, University of Iceland, Reykjavik, Iceland, [2]Institute for Rock Magnetism, University of Minnesota, Minneapolis, MN, United States, [3]School of Earth and Environment, University of Leeds, Leeds, United Kingdom

Fires are an integral part of many terrestrial ecosystems and have a strong impact on soil properties. While reports of topsoil magnetic enhancement after fires vary widely, recent evidence suggests that plant ashes provide the most significant source of magnetic enhancement after burning. To investigate the magnetic properties of burnt plant material, samples of individual plant species from Iceland and Germany were cleaned and combusted at various temperatures prior to rock magnetic and geochemical characterization. Mass-normalized saturation magnetization values for burnt plant residues increase with the extent of burning in nearly all samples. However, when normalized to the loss on ignition, fewer than half of ash and charcoal samples display magnetic enhancement relative to intact plant material. Thus, while magnetic mineral concentrations generally increase, changes in the total amount of magnetic material are much more variable. Elemental analyses of Icelandic samples reveal that both total plant Fe and saturation magnetization are strongly correlated with Ti and Al, indicating that most of the Fe-bearing magnetic phases originate from inorganic material such as soil and atmospheric dust. Electron microscopy confirmed that inorganic particulate matter remains on most plant surfaces after cleaning. Plants with more textured leaf surfaces retain more dust, and ash from these samples tend to exhibit higher saturation magnetization and metal concentrations. Magnetic properties of plant ash therefore result from the thermal transformation of Fe in both organic compounds and inorganic particulate matter, which become concentrated on a mass basis when organic matter is combusted. These results indicate that the soil magnetic response to burning will vary among sites and regions as a function of 1) fire intensity, 2) the local composition of dust and soil particles on leaf surfaces, and 3) vegetation type and consequent differences in leaf morphologies.

Keywords: soils, rock magnetism, vegetation, soil magnetism, fire

OPEN ACCESS

Edited by:
Sara Satolli, G.d'Annunzio University of Chieti and Pescara, Italy

Reviewed by:
Aldo Winkler, Istituto Nazionale di Geofisica e Vulcanologia (INGV), Italy
Neli Jordanova, National Institute of Geophysics, Geodesy and Geography (BAS), Bulgaria
Eduard Petrovsky, Institute of Geophysics (ASCR), Czechia

***Correspondence:**
Jessica L. Till
jtill@hi.is

Specialty section:
This article was submitted to Geomagnetism and Paleomagnetism, a section of the journal Frontiers in Earth Science

Received: *07 August 2020*
Accepted: *04 November 2020*
Published: *12 January 2021*

Citation:
Till JL, Moskowitz B and Poulton SW (2021) Magnetic Properties of Plant Ashes and Their Influence on Magnetic Signatures of Fire in Soils. Front. Earth Sci. 8:592659. doi: 10.3389/feart.2020.592659

1 INTRODUCTION

Wildfires and anthropogenic burning affect many aspects of soils, including their magnetic properties. Wildfires have long been suggested as a possible source of topsoil magnetic enhancement (e.g., Le Borgne, 1960; Kletetschka and Banerjee, 1995) and many examples of increased magnetic susceptibility following fires have been observed (Clement et al., 2011;

Jordanova et al., 2019a). Because magnetic enhancement in soils relative to unweathered parent material often correlates closely with various environmental factors (Maher et al., 2003), understanding the impact of fires on soil magnetism is important for accurate interpretation of magnetic paleoenvironmental proxies.

Fire-induced magnetic enhancement may occur through thermal transformation of weakly magnetic ferric oxide and oxyhydroxide soil minerals such as ferrihydrite, lepidocrocite, goethite, and hematite (Hanesch et al., 2006; Till et al., 2014; Jiang et al., 2018; Till and Nowaczyk, 2018) to strongly magnetic phases such as magnetite or maghemite. Such reactions likely contribute to the enhanced magnetic susceptibility observed in some burnt soils compared with unburnt soils (Gedye et al., 2000; Blake et al., 2006), particularly in forest fires and similar high-intensity burning events. By contrast, a study by Roman et al. (2013) on grassland fire temperatures concluded that fire is an unlikely source of significant magnetic enhancement in prairie soils based on the relatively low temperatures experienced by the soil compared with temperatures necessary to produce mineralogical changes during laboratory heating.

Another potential source of pyrogenic magnetic minerals is the plant ash itself. Several archeological studies have noted that ashes from wood and other plant-based fuel sources often contain high concentrations of magnetic minerals relative to soils (Peters et al., 2001; Peters and Batt, 2002; Church et al., 2007), a feature that is sometimes exploited for archaeological surveying (McClean and Kean, 1993). One of the few investigations of plant ash magnetic properties was conducted by Lu et al. (2000), who determined that the magnetic susceptibility of plant ash exceeds that of many well-developed soils. They further concluded that only about half of the soil magnetic enhancement in natural burn sites could be attributed to mineralogical changes due to heating of the soil. Petrovský et al. (2018) studied magnetic susceptibility of forest soils that had been fertilized by wood ash, noting that the ash contained significant concentrations of superparamagnetic ferromagnetic particles that persisted in the soil following wood ash addition. Similarly, Jordanova et al. (2018) argued that plant ashes were the source of enhanced topsoil magnetic susceptibility following forest fires, which was typically observed in the uppermost few cm.

However, the source of magnetism in plant ash has never been investigated in detail and only limited magnetic data has been reported for ash material. This study presents a detailed analysis of changes in magnetic properties that accompany burning of plant materials. Using burnt residues from known species, we synthesize rock magnetic properties with geochemical data and microscopy observations to identify the likely origin of magnetic material in plant-derived ash and char deposits to better understand how soil and sediment magnetic properties reflect vegetation burning.

2 METHODS

2.1 Sample Collection and Preparation

Recently fallen litter and senescent plant material was collected from over 20 plant genera (see **Table 1**) in the Reykjavik Botanical Garden in autumn of 2017 and 2018. Depending on the plant type, materials collected included dead leaves or needles, shoots, cones, stems and woody litter, flowers, and seeds. Green leaves were also collected from selected plant types to investigate potential seasonal effects on the composition of plant ash. *Lupinus nootkatensis* plants (leaves, flowers, seeds, stems) were sampled in summer and autumn of 2017 from the Borgarfjordir region in western Iceland. Additional cleaned and milled plant samples were prepared and provided by the Leibniz Centre for Agricultural Landscape Research (ZALF), Germany. Specimen details and sampling locations are given in **Table 1**.

Most Icelandic plant samples were cleaned shortly after collection by agitating vigorously in a solution of 0.1 (v/v) Triton X-100 biological detergent followed by thoroughly rinsing in water. Cleaned samples were then oven-dried at 70°C for 24–48 h and gently crushed. Subsets from several selected samples were dried directly after collection without cleaning to determine the effect of washing on magnetic properties. 2–4 g of dried plant material were combusted in ceramic crucibles in a muffle furnace at 200 and 300°C for 6 h to produce char and at 550°C for 4 h to produce ash. Sample and crucible masses were measured immediately before and after heating to determine loss-on-ignition values. Multiple batches of ash were produced for most plant samples, which were pooled. For these samples, the LOI represents an average across ash specimens. The percent of mass remaining after combustion is given for each sample in **Supplementary Table S1**.

Small amounts (30–100 mg) of ash, char, or intact plant material were ground to powder and firmly packed into gelatin capsules with quartz wool for hysteresis and low-temperature magnetic measurements.

2.2 Magnetic Measurements and Sample Characterization

Thermomagnetic measurements were made on selected ash and char samples to identify characteristic Curie temperatures (T_C) of the main magnetic phases. Susceptibility was measured from room temperature up to either 650 or 700°C and again on cooling to 50°C on a low-field AC susceptometer (Kappabridge KLY-3) in flowing Ar gas. A small number of thermomagnetic curves were run in air, and these generally exhibited more irreversible behavior than measurements in Ar, indicating that the burnt samples contain phases sensitive to oxygen. Curie temperatures were determined by plotting the derivative of each susceptibility curve on heating, where the temperature at the minimum in the derivative curve was taken as T_C, as discussed in Petrovský and Kapička (2006); Fabian et al. (2013).

Low temperature magnetization and AC susceptibility (χ) were obtained with a superconducting quantum interference device (SQUID) magnetometer (Quantum Design, San Diego, CA, United states – MPMS). Low-temperature remanence properties can reveal diagnostic phase transitions in certain magnetic minerals as well as providing information about magnetic domain states, and hence, grain size. Magnetization measurements follow the FC-ZFC-LTSIRM-RTSIRM LTD

TABLE 1 | List of plant species and sampling details.

Scientific name	Sampling location	Plant parts collected
Alchemilla alpina	Reykavik Botanical Garden, Iceland	Dead leaves and flowers
Athyrium felix-femina	Reykavik Botanical Garden, Iceland	Green and dead leaves and stems
Avenula pubescens	Reykavik Botanical Garden, Iceland	Dead leaves and seeds
Betula pubescens	Reykavik Botanical Garden, Iceland	Leaf litter
Carex nigra	Reykavik Botanical Garden, Iceland	Dead leaves
Deschampsia cespitosa	Reykavik Botanical Garden, Iceland	Dead leaves and seeds
Equisetum sylvaticum	Reykavik Botanical Garden, Iceland	Dead leaves and stems
Juniperis communis	Reykavik Botanical Garden, Iceland	Needles and woody litter
Leymus arenarius	Reykavik Botanical Garden, Iceland	Green and dead leaves and seeds
Picea sitchensis	Reykavik Botanical Garden, Iceland	Needles, cones, and woody litter
Pinus contorta	Reykavik Botanical Garden, Iceland	Needles, cones, and woody litter
Populus trichocarpa	Reykavik Botanical Garden, Iceland	Green leaves and leaf and woody litter
Ranunculus repens	Reykavik Botanical Garden, Iceland	Green and dead leaves
Rumex longifolius	Reykavik Botanical Garden, Iceland	Seeds and stems
Salix caprea	Reykavik Botanical Garden, Iceland	Leaf litter
Sorbus decora	Reykavik Botanical Garden, Iceland	Leaf litter
Trifolium pratense	Reykavik Botanical Garden, Iceland	Green and dead leaves, stems and flowers
Lupinus nootkatensis	Fossatún valley, western Iceland	Fresh and dead leaves, flowers, seeds, and stems
Calamagrostis epigejos	Russendamm, Lower Odra Valley, Germany	Green leaves
Zea mays	Dedelow, Germany	Stover
Fagus sylvatica	Beerenbusch, Germany	Leaf litter
Festuca arundinacea	Paulinenaue, Germany	Green leaves
Cirsium arvense	Paulinenaue, Germany	Green leaves and flowers
Phalaris arundinacea	Criewen, Lower Odra Valley, Germany	Green leaves

measurement protocol from Bilardello and Jackson (2013). Low-temperature saturation isothermal remanent magnetization (LTSIRM) was acquired as a field-cooled (FC) and zero-field-cooled (ZFC) magnetization by cooling to 10 K in either a 2.5 T field or in zero-field. At 10 K, a 2.5 T field was applied and then reduced to zero (<1 μT) and magnetization was measured during warming to 300 K in 5 K steps. Following the FC-ZFC measurements, a 2.5 T field was applied and then reduced to zero at 300 K imparting a remanent magnetization (RTSIRM). The RTSIRM curve was measured during cooling to 10 K and subsequent warming back to 300 K at 5 K increments. In-phase (χ') and quadrature (χ'') magnetic susceptibility was measured in an AC field with a peak amplitude of 0.3 mT at 1, 10, and 100 Hz on warming from 10 to 300 K. To estimate the presence of ultrafine-grained superparamagnetic particles, frequency dependence was calculated from the room-temperature susceptibility values as: $X_{fd} = 100(X_{lf}–X_{hf})/X_{lf}$, where X_{lf} and X_{hf} are the susceptibilities at low and high frequencies (1 and 100 Hz), respectively.

Hysteresis loops at room temperature were measured up to a maximum field of 1 T on a Princeton Corporation Measurements vibrating sample magnetometer at the Institute of Rock Magnetism at the University of Minnesota (United States) to constrain the domain state and grain size distributions of magnetic remanence carriers in the specimens. Averaging times ranged from 100 ms for ash to 500 ms for unburnt plant samples. Backfield remanence (DC demagnetization) curves were also measured for most samples up to −500 mT after saturation in a 1 T field. Saturation magnetization (M_S), saturation remanent magnetization (M_R), coercivity (H_c), and high-field susceptibility (X_{HF}) values were determined from hysteresis loops after subtracting the high-field slope over the interval of 0.7–1.0 T using the nonlinear approach-to-saturation fitting method of Jackson and Solheid (2010). All hysteresis parameters in figures and tables represent slope-corrected data. The M_S values in **Supplementary Table S1** are normalized by the specimen mass, which is a good indicator of ferromagnetic mineral concentrations in the sample. However, it is also useful to view M_S values when normalized by the initial plant mass before burning because the mass of the system is not constant during combustion. This allows us to see how the total amount of ferromagnetic material in the system changes during burning.

Selected plant samples were mounted on carbon adhesive discs and carbon-coated for scanning electron microscopy characterization using a Hitachi tabletop SEM with a LaB^6 filament equipped with an energy dispersive X-ray detector. Magnetic extracts from representative Icelandic ash samples were also prepared and imaged in the same way.

Total element compositions of Icelandic plant ash samples were analyzed via ICP-OES after extraction with HNO^3-HF-$HClO^4$-H^3BO^3, following the procedure outlined in Xiong et al. (2019). In brief, samples were ashed at 550°C and then dissolved in HNO^3-HF-$HClO^4$. After evaporation to dryness, H^3BO^3 was added to the samples and evaporated to dryness to ensure re-dissolution of aluminum salts. Finally, samples were re-dissolved in warm 6N HCl. No residue remained after this procedure. We used an international sediment standard (PACS-2) to test the procedure to ensure full extraction of mineral phases. Replicate extractions of this standard gave recoveries of >95% for all elements of interest, with RSDs of <2%.

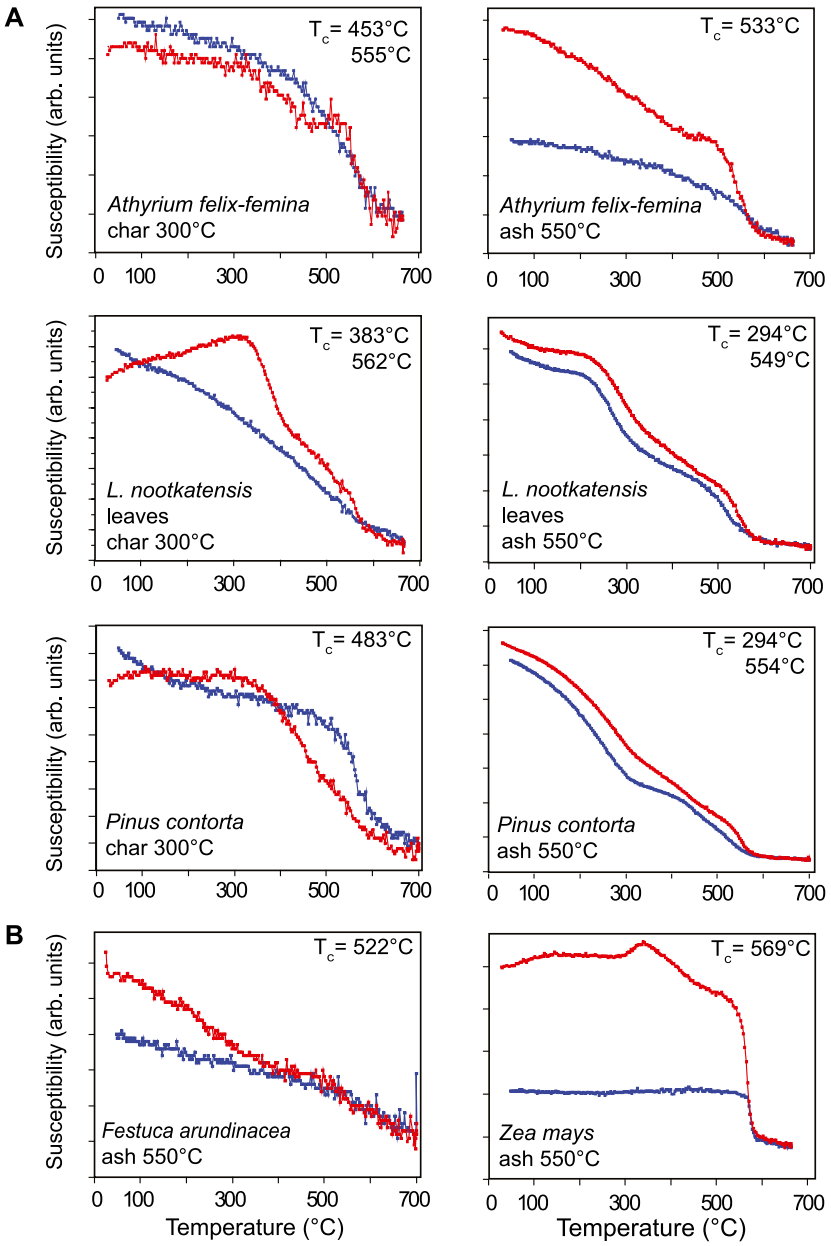

FIGURE 1 | Example thermomagnetic curves of susceptibility measured on warming (red) and cooling (blue) for selected ash and char from **(A)** Icelandic plant litter and **(B)** German plant samples.

3 RESULTS

3.1 Thermomagnetic Behavior

Thermomagnetic curves for plant char and ash from Icelandic samples nearly all exhibit a drop in bulk susceptibility between 560 and 580°C, consistent with the Curie temperature (T_C) of magnetite (**Figure 1A**). Several Icelandic samples also indicate the presence of a phase with a T_C around 300°C. In general, the shape of the χ vs. T curves are different for char and ash produced from the same plant sample, suggesting that heating to the higher temperatures used for ashing produces magnetic phases with somewhat different compositions than those resulting from lower temperature treatments. By contrast, ash from the German plant samples display continuous decreases in susceptibility with heating and do not exhibit distinct disordering temperatures, except for *Zea mays*, which has a pronounced Curie temperature around 580°C (**Figure 1B**). No clear evidence of hematite or maghemite was observed in either high- or low-temperature magnetic data.

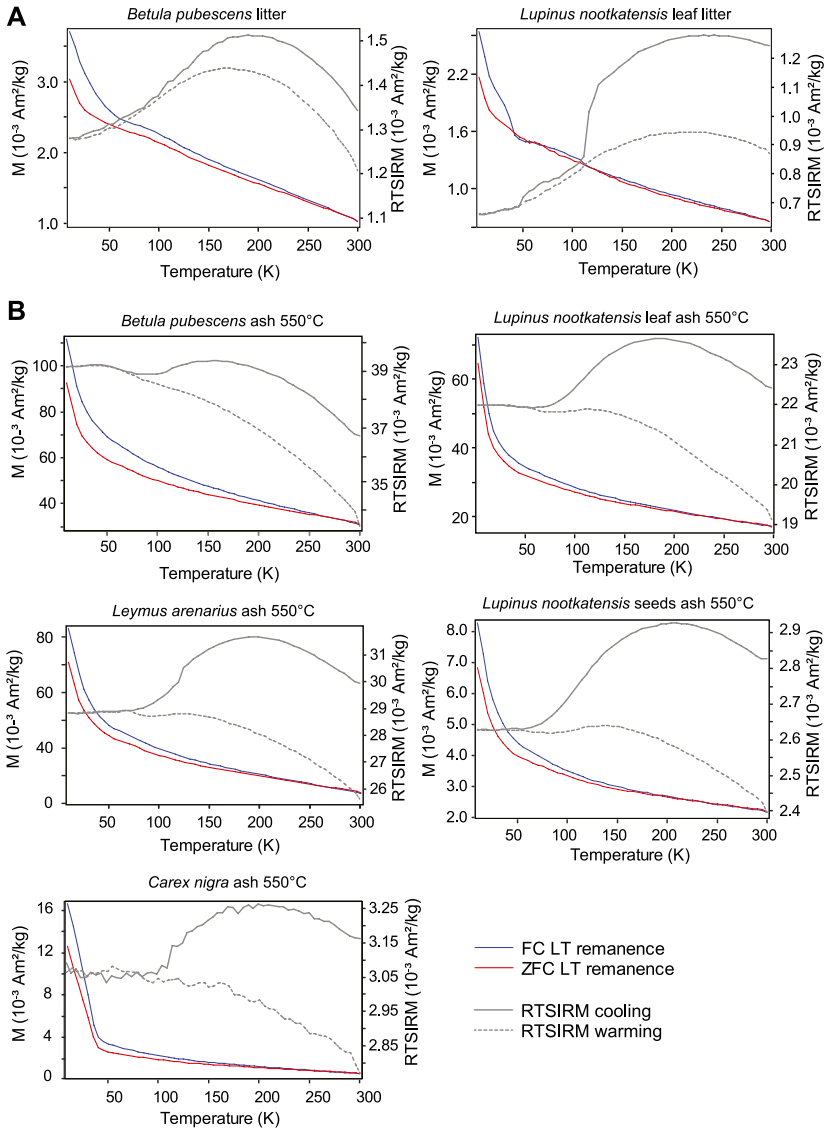

FIGURE 2 | Low-temperature remanence measurements after field-cooling (FC) and zero-field cooling (ZFC) along with cooling and warming curves of room-temperature remanence (right-hand scales) for **(A)** unheated Icelandic plant litter and **(B)** ashed Icelandic litter samples.

3.2 Low-Temperature Magnetic Properties

Low temperature magnetization curves (FC, ZFC, and RTSIRM) were measured for several sets of unburned, char and ash samples. In general, the FC and ZFC curves for Icelandic and German samples showed a steady decay of remanence on warming from 15 to 300 K, indicative of progressive unblocking of superparamagnetic nanoparticles. There were weak indications of the Verwey transition (T ~ 100–120 K) for magnetite (**Figure 2A**) for the unburnt forms but no indication after combustion at 550°C. The exception was *Zea mays* (Germany) after charring at 300°C which had a noticeable expression of the Verwey transition on warming (**Figure 3A**). For two other samples from Iceland (*Betula pubsescens* and *Lupinus nootkatensis*), the unburned samples also indicated a magnetic transition near 40–50 K, but this disappeared once the samples were reduced to ash. However, the presence of magnetite in all samples (unburned, char, and ash) was confirmed from RTSIRM measurements on cooling from 300 K, which showed the characteristic magnetic signature for the Verwey transition (**Figure 2B**). In addition, hump-shaped remanence curves observed on cooling suggested that some of the magnetite was likely partially oxidized (Özdemir and Dunlop, 2010). For all samples measured there was no indication of the Morin transition (T ~ 260 K) associated with hematite in any the FC, ZFC, or RTSIRM curves. Several of the measurements made on cooling after imparting a RTSIRM exhibit sharp drops around 150 K. These are considered to be artifacts that occurred due to shifting of the capsule in the sample holder. Data in **Figure 2** have been adjusted to correct for this artifact, while the raw measurements are included in the **Supplementary Table S3**.

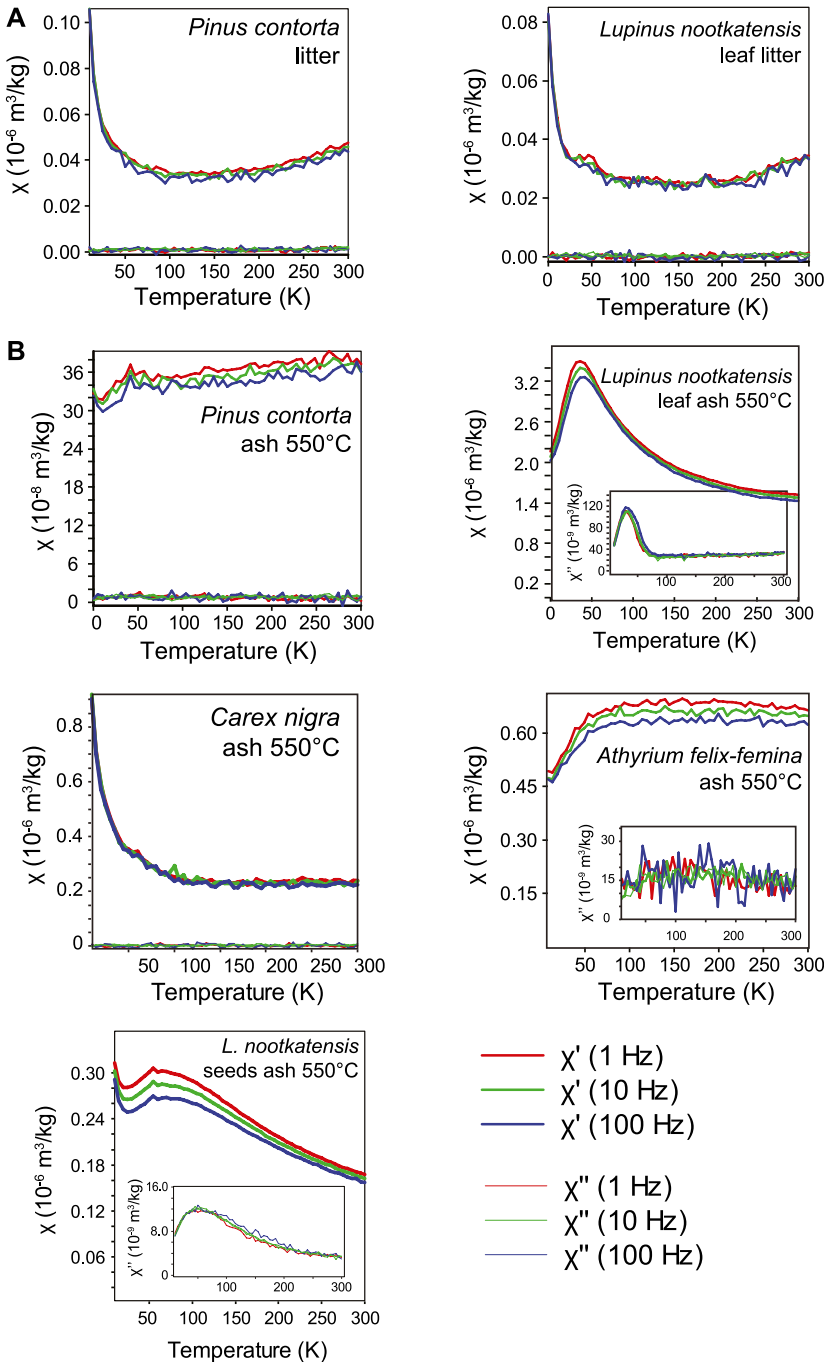

FIGURE 3 | Low-temperature measurements of **(A)** FC-ZFC and RTSIRM remanence and **(B)** frequency-dependent susceptibility for German char and ash samples.

The temperature and frequency dependence of AC susceptibility (χ', χ'') for selected samples show a combination of paramagnetic and ferrimagnetic behavior (**Figures 3** and **4**). Unburnt samples displayed paramagnetic behavior ($\chi' \propto 1/T$) at the lowest measurement temperatures with a rapid decrease in χ' with increasing temperature until around 150–200 K, when susceptibility begins to level off or increase slightly due to the ferrimagnetic contribution from magnetite. In this temperature range, some frequency dependence of susceptibility was observed, but the out-of-phase susceptibility was near zero with no temperature-dependent behavior. There was no clear indication in the χ-T curves of magnetite.

After combustion and transformation to char or ash, significant changes in susceptibility behavior occurred, with

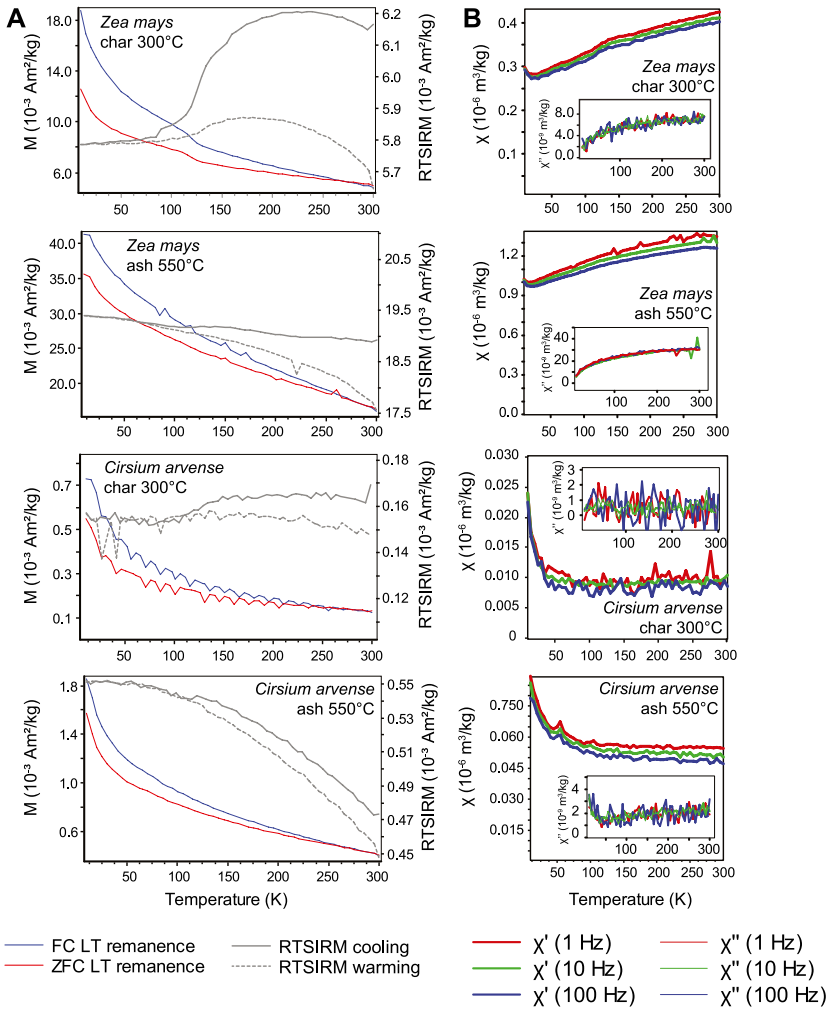

FIGURE 4 | Low-temperature frequency-dependent susceptibility measurements for **(A)** Icelandic litter and **(B)** Icelandic ash samples. Out-of-phase susceptibility measurements are shown in inset plots.

the exception being the ash from *Carex nigra* which displayed pure paramagnetic behavior. The most noticeable changes occurred for ash from *Lupinus nootkatensis* and *Betula pubsescens*, where paramagnetic behavior is replaced by frequency dependent susceptibility and thermal relaxation peaks at T ~40–50 K in both χ' and χ'', characteristic of superparamagnetism in nanoparticles. In contrast to relaxation peaks, ash samples from *Pinus contorta* and *Athyrium felix-femina* displayed an increase in susceptibility from 15 to 50 K followed by gradual increase in χ'(T) to 300 K. For both *Pinus contorta* and *Athyrium felix-femina*, χ'' was near zero and showed no temperature-dependent behavior.

The char and ash samples of *Zea mays* show similar χ-T behavior with a small paramagnetic tail below 20 K followed by steady increase in susceptibility to 300 K. The Verwey transition is seen in the sample charred at 300°C but is absent in the ash sample, similar to the FC-ZFC results. There is also both frequency dependence and a monotonically increasing temperature dependent χ''(T) over the entire temperature range. Unlike *Zea mays*, χ-T curves for char and ash samples of *Cirsium arvense* displayed stronger paramagnetic behavior. Frequency-dependent behavior and temperature-dependent χ'' was seen only for the ash sample.

Low-field room-temperature susceptibility values obtained from the MPMS measurements indicate that bulk susceptibilities for fresh litter and 200°C char are in the range 7.0×10^{-8}–1.3×10^{-7} m^3/kg, while the 300°C char in the range 2.3×10^{-8}–2.3×10^{-6} m^3/kg, and values for ash are in the range 7.9×10^{-8}–2.8×10^{-6} m^3/kg. Frequency dependence of susceptibility is generally higher than than in char or unburnt litter samples, reaching 7.1% in ash from Icelandic plants and as much as nearly 12% in the German sample *Cirsium arvense*. The bulk susceptibilities for our ash samples are very similar to the range values reported for wood ash and cigarette ashes by Jordanova et al. (2006). They also reported X_{fd} values ranging from 5.0 to 8.5%, which is consistent with the range of values observed in this study. The highest susceptibilities in our Icelandic samples are lower than the average value of

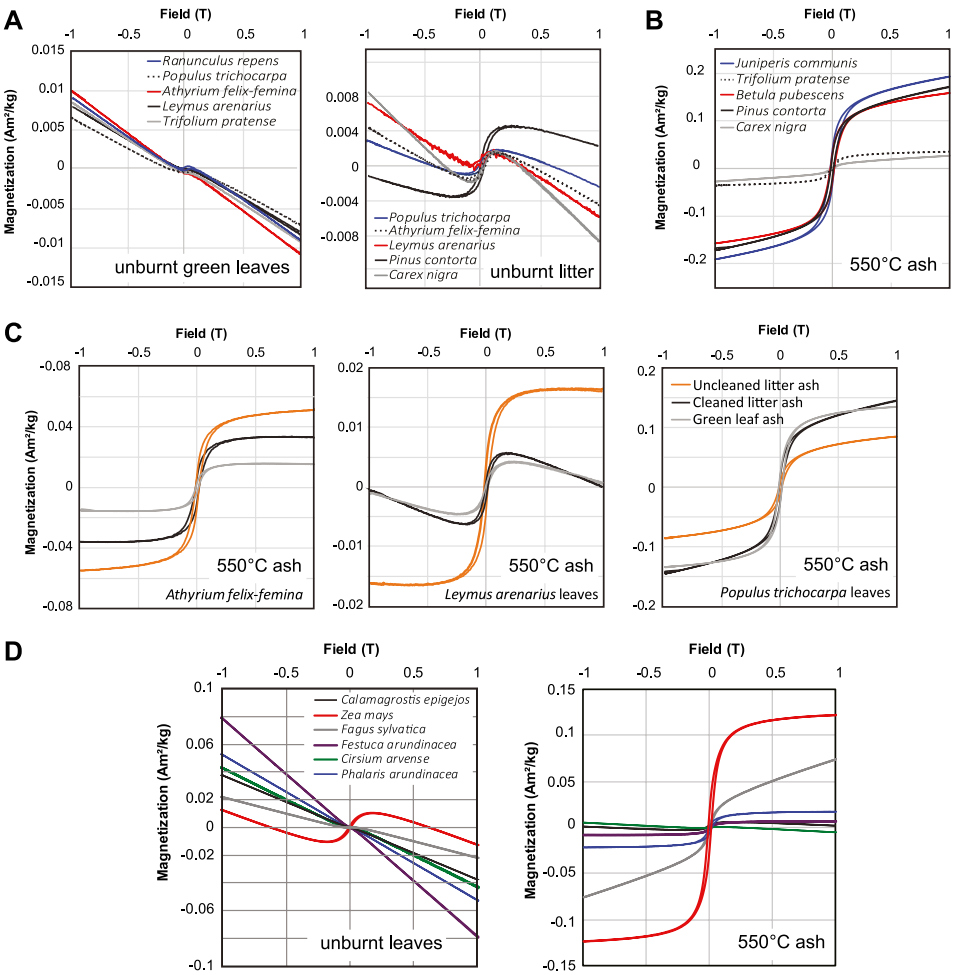

FIGURE 5 | Example hysteresis loops for **(A)** unburnt Icelandic plant samples, **(B,C)** ashed Icelandic plants, and **(D)** unburnt and ashed German plant samples.

5.3×10^{-6} m^3/kg reported for ash from C4 plants from China by Lu et al. (2000). It is also worth noting that the average susceptibility of ash from C3 plants studied by Lu et al. (2000) was significantly lower at 1.2×10^{-6} m^3/kg.

3.3 Hysteresis Properties

Hysteresis loops of unburned plant samples from both Iceland and Germany are dominantly characterized by diamagnetic high-field slopes with a superimposed ferromagnetic signal of variable strength (**Figures 5A,D**). Green leaves have notably smaller ferromagnetic components compared with dead leaves and plant litter samples. The diamagnetic background becomes reduced after burning at 300 and 550°C, with most ash samples having a dominantly ferromagnetic character and a small paramagnetic high-field slope. Several samples charred at 200°C had no discernible ferromagnetic component or the signal-to-noize ratios were not sufficient to confidently resolve hysteresis parameters, even in plants for which unburnt litter samples exhibited measurable hysteresis.

Ash from litter samples that were not cleaned before burning have consistently higher M_s compared to ash from cleaned litter (**Figure 5C**), however, the hysteresis loop shapes are nearly identical. Hysteresis parameters of ash and char from cleaned samples cannot be distinguished from uncleaned plant samples in plots of squareness (M_R/M_s) vs. H_C (**Figure 6A**). However, char and ash from green Icelandic plants and German plant samples have overall lower coercivities and M_R/M_s ratios. The majority of measured plant samples fall in between the compositional trends proposed by Wang and Van der Voo (2004) for Ti-free magnetite (TM0) and TM60 titanomagnetite (**Figure 6A**), although several samples plot close to the magnetite trend. Icelandic samples charred at 300°C exhibit somewhat lower coercivities than unburnt samples or ash and char from other temperatures (**Supplementary Table S1**), but otherwise M_R/M_s and H_C do not exhibit a clear dependence on burning temperature suggestive of a systematic change in domain state.

Saturation magnetization values of ash and char vary significantly among plant types for all burning temperatures. A comparison of mass-normalized M_s (based on the mass of the burnt samples) as a function of combustion temperature is shown in **Figure 7** for both Icelandic and German samples relative to the unburnt plants. After charring at 200°C, M_s either decreases or

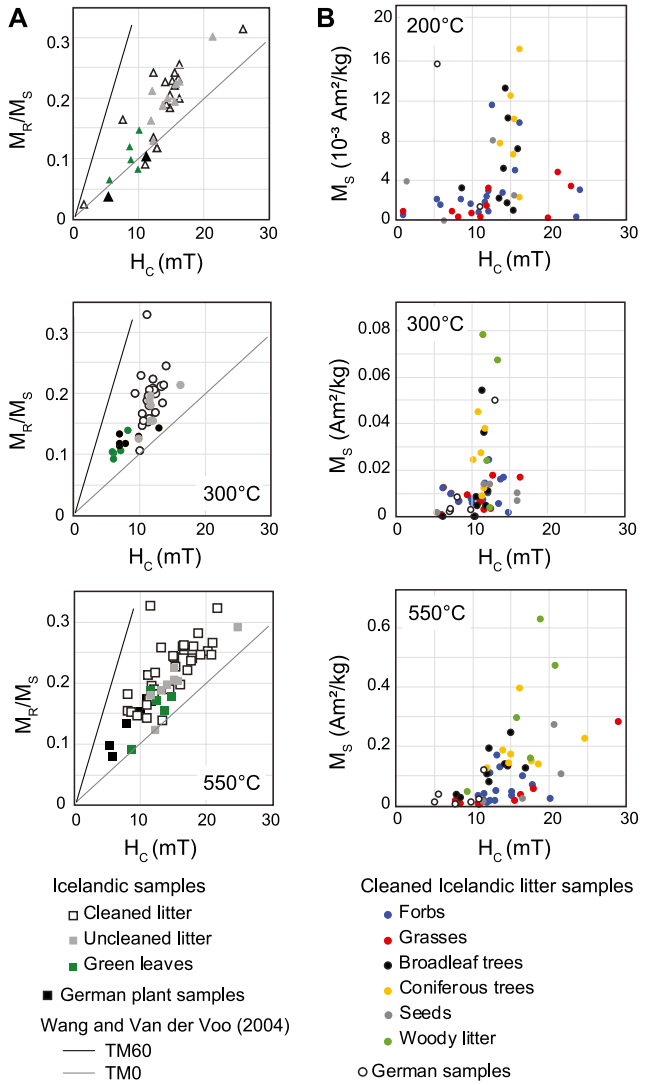

FIGURE 6 | (A) Hysteresis squareness (M_R/M_s vs. H_c plots for ash and char from different subsets of plant samples along with compositional trends proposed by Wang and Van der Voo (2004). **(B)** Variations in saturation magnetization vs. coercivity by plant type for ash and char from cleaned Icelandic litter samples.

remains relatively unchanged for most samples, while the majority of samples burnt at 300 and 550°C exhibit elevated M_s (**Figure 7A**). Ash from Icelandic litter samples exhibit M_s values that are higher than those of the unburnt litter by a factor ranging from approximately 2–35. By contrast, ash from green Icelandic samples are enhanced by as much as a factor of 160, while ash from German samples display more moderate enhancements, up to a factor of 16 (**Figure 7D**). The pattern of changes in M_s with burning temperature for uncleaned Iceland litter samples are generally very similar to those of the cleaned litter samples (**Figure 7C**).

Average loss-on-ignition values after burning at 200°, 300°, and 550°C were 26%, 78%, and 93%, respectively, for Icelandic litter and German samples. Green leaf samples from Iceland had LOI values of 39%, 68% and 91%, respectively (**Supplementary Table S1**). To examine the relationship between LOI and magnetic properties of ash and char, hysteresis parameters are plotted as a function of mass remaining after burning in **Figure 8**. To account for the effect of mass loss during burning on the mass-normalized M_s values, we also calculated saturation magnetization values using the initial mass of plant material prior to burning based on the measured LOI values for each sample. When these values are plotted relative to that of the unburnt plant material, the changes in M_s as a function of burning temperature are much more variable. Approximately half of the samples exhibit decreases in M_s after ashing at 550°C while M_s increases by up to a factor of 2.3 in the remaining samples. However, ash from certain green Icelandic plant samples exhibit sharply enhanced M_s even after accounting for the LOI (**Figure 7B**). M_s is similarly lower in char and ash for most German plant samples when normalized by the initial plant mass.

3.4 Composition and Surface Features of Plant Material

Total concentrations of Fe, Ti and Al determined from complete digestion of ash from cleaned Icelandic plant litter samples are shown in **Figure 9A** and listed in **Supplementary Table S2**, along with other selected metal concentrations. Among the plant species sampled, Fe and Ti contents vary by approximately 20-fold, with Fe concentrations in ash ranging from 3.9 to 71.5 mg/g. Total Fe is strongly correlated with both Ti and Al but is poorly correlated with micronutrients such as Mg, Mn, Cu, and Zn (see Supplemental Data). Saturation magnetization values in ash samples (burnt at 550°C) also exhibit a slightly weaker but clear positive correlation with Ti content (**Figure 9B**). Ti (and to a lesser extent Al) in plant tissues is commonly considered an indicator of soil and dust inclusion in plants, as Ti is not present at appreciable levels in most biological materials but is abundant in soils and atmospheric dust, as well as in particulate matter from pollution sources (Cherney and Robinson, 1983; Cary et al., 1986; Cook et al., 2009). The close correlations between Fe and both Ti and Al in the Icelandic ash samples suggest that a significant proportion of the Fe is from inorganic sources.

Jóhannesson et al. (2007) reported Fe concentrations in a range of 57–1,379 ppm in grasses and other forage plants from nearly 50 Icelandic farms. Similarly, Eiríksson et al. (2010) found an even wider variation of Fe contents in Iceland forage, from 100 to 5,000 ppm. These previous analyses are consistent with our determined elemental compositions in ash, which correspond to Fe contents in dry plant matter in the range 221–4,531 ppm. In an overview of chemical compositions of biomass, Vassilev et al. (2010) gives mean values of Fe, Ti, and Al contents in various forms of plant material that fall in the middle of the values observed for our Icelandic ash samples (**Figure 9A**), and with very similar elemental ratios to those reported here. Vassilev et al. (2010) further notes that strong correlations exist among Fe, Ti, Si, Na, and Al among various forms of biomass, and that significant Al concentrations are usually regarded as an indicator of soil inclusion.

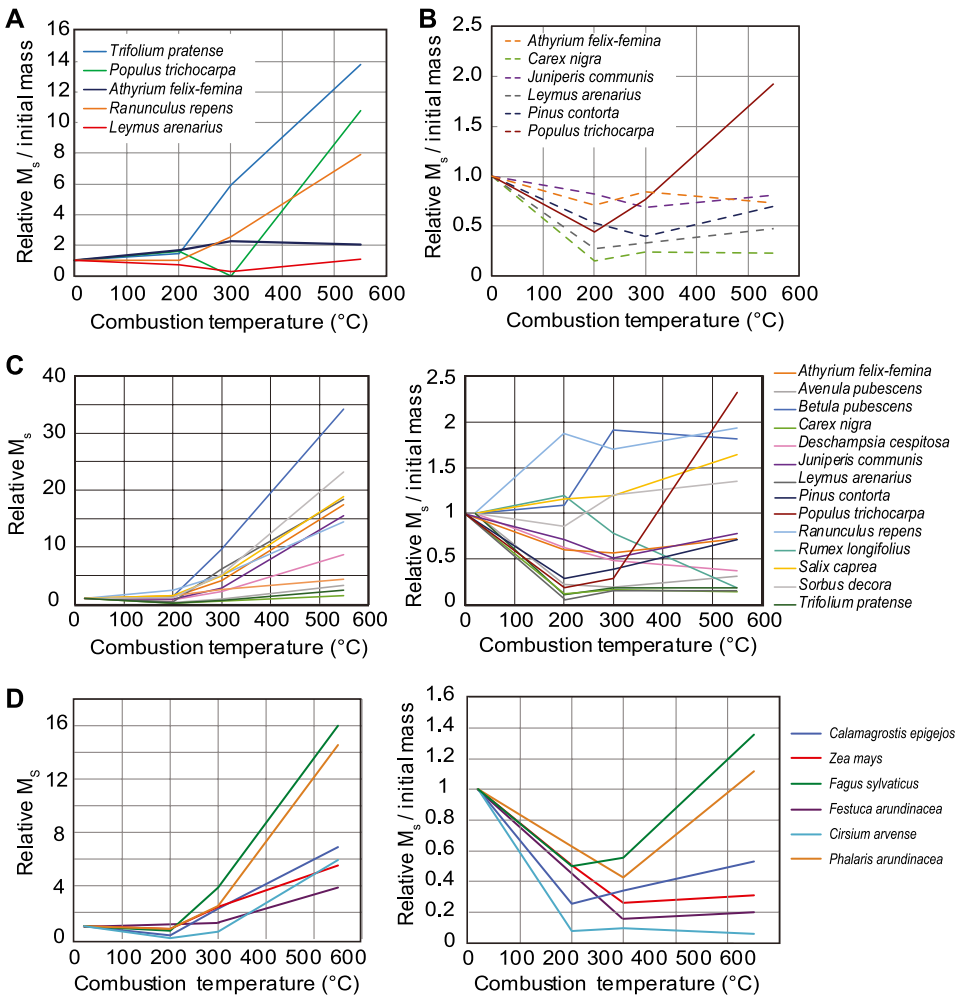

FIGURE 7 | Changes in saturation magnetization values in ash and char with burning relative to unburnt material for **(A)** green leaves from Icelandic plants, **(B)** uncleaned Icelandic plant litter, **(C)** cleaned Icelandic plant litter, and **(D)** German plant samples. Lefthand plots in C and D show M_s normalized by ash/char sample mass after burning while the righthand plots, as well as those in A and B, indicate relative M_s normalized by the initial plant mass prior to burning.

Examination of cleaned plant samples with SEM imaging prior to burning revealed variable quantities of particulate matter on plant surfaces (**Figure 10A**). These particles appear as bright phases in backscattered electron imaging mode, and are interpreted to be fine inorganic dust and soil material that remain entrained in the leaf surfaces after cleaning. Based on these images, we inferred a qualitative relationship between leaf texture and particulate matter content. For example, large amounts of particulate matter are embedded in the thick, waxy cuticle on needles of conifer species such as Sitka spruce (*Picea sitchensis*, **Figure 10A**). Similarly, the fine leaf hairs of downy birch (*Betula pubescens*) are also effective in trapping particles on the leaf surface. By contrast, black sedge (*Carex nigra*) has a relatively smooth leaf surface with little inorganic material. Particulate matter was also observed on the surface of German plant samples, especially *Zea mays*. Energy dispersive spectroscopy (EDS) maps of Fe and Ti in magnetic extracts from selected Icelandic ash samples are shown in **Figure 10B**. The majority of Fe-rich grains in these samples are associated with Ti, and these are assumed to be derived from lithogenic titanomagnetite in the basaltic soil and dust parent materials.

4 DISCUSSION

4.1 Possible Domain States of Magnetic Carriers in Ash

Most previous studies investigating magnetic properties of pyrogenic magnetic phases have found evidence for predominantly fine-grained magnetite of SD or SP-size. Kent et al. (2017) interpreted a unit enriched in isolated SD magnetite particles in continental shelf deposits as representing increased wildfire occurrence on land. In a simulated archeological burn, Carrancho and Villalaín (2011) observed the formation of SD magnetite across the heated surface of an experimental hearth. Similarly, Oldfield and Crowther (2007) found that pyrogenic

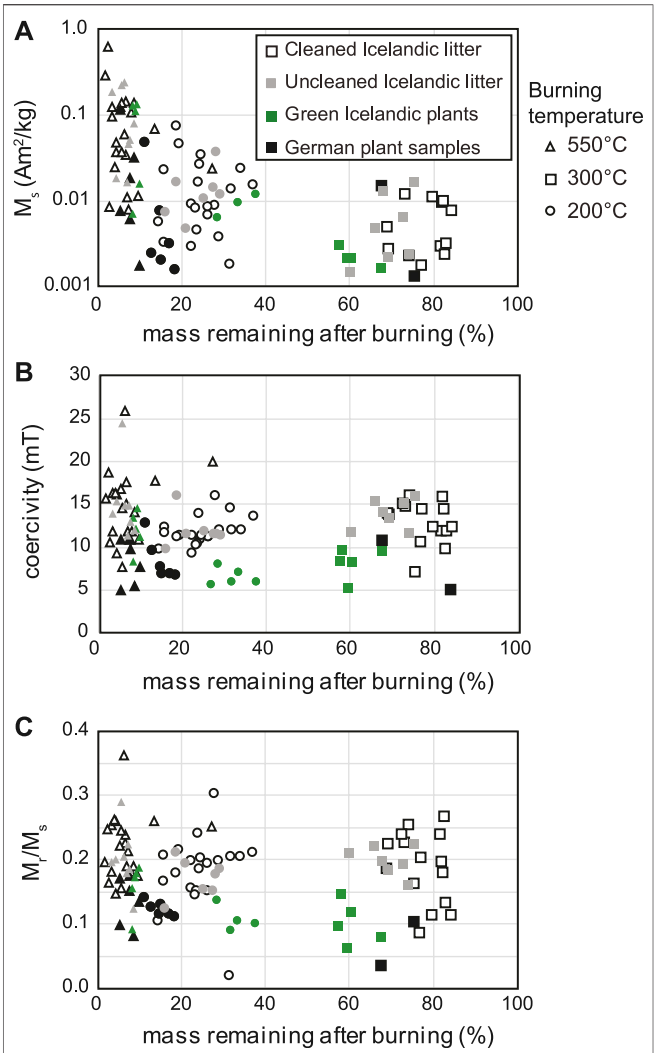

FIGURE 8 | Hysteresis parameters as a function of % mass remaining after burning. **(A)** Saturation magnetization, **(B)** coercivity, and **(C)** (M_R/M_s) of ash and char from different subsets of plant samples. Note that the vertical axis in A is plotted on a logarithmic scale.

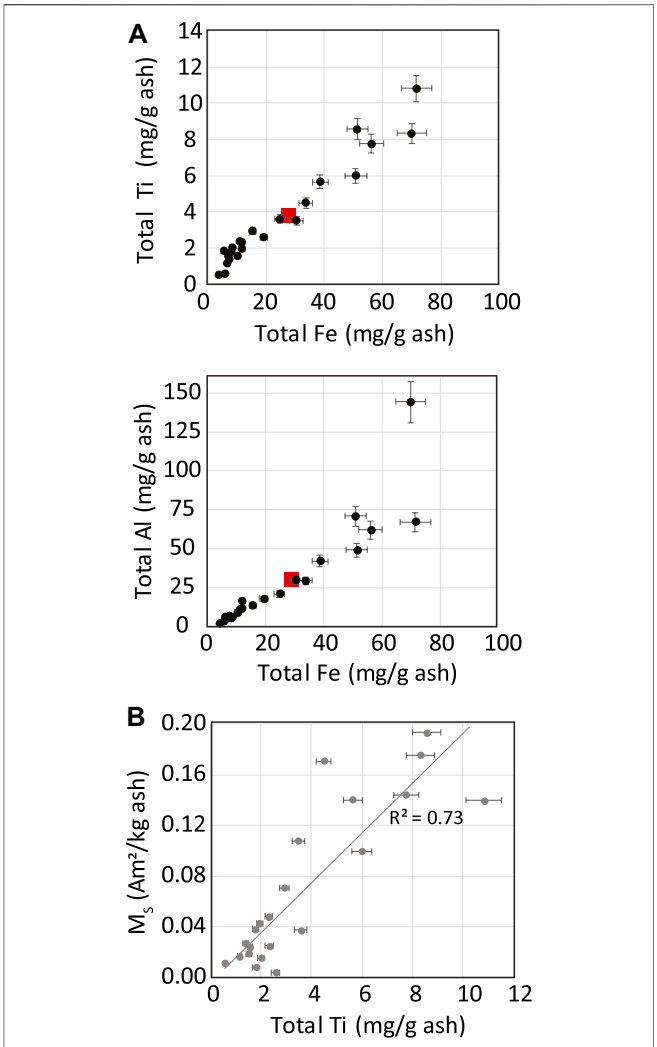

FIGURE 9 | (A) Concentrations of Fe plotted against Al and Ti in Icelandic plant ash samples determined by wet digestion. **(B)** Comparison of Ti content with saturation magnetization based on the ashed mass of Icelandic plants. Error bars are based on relative standard deviation among analytical replicates. Data shown are for samples combusted at 550°C for 4 h. Red symbols in A represent mean elemental concentrations in various forms of biomass reported by Vassilev et al. (2010).

ferrimagnetic phases are characteristically finer grained than typical pedogenic ferrimagnetic mineral assemblages. While we observed relatively large, MD-sized particles in SEM analysis of magnetic extracts from the ash, the elevated coercivities and moderately strong frequency dependence of susceptibility in many of the ash samples also suggests that there is likely a significant component of fine-grained SD and SP-sized magnetite as well.

In our low-temperature remanence measurements, the FC and ZFC curves for ash samples do not exactly correspond to the behavior expected for SD magnetite. For SD magnetite, FC and ZFC curves are typically bifurcated only below the Verwey transition (T_v), while merging together above T_v. In the data shown in **Figures 2** and **3**, the separation between FC and ZFC curves extends almost over the entire temperature range of measurement (20 –300 K) and, therefore, is not a clear indicator of pure SD magnetite. This type of behavior is observed in non-SD sized titanomagnetites and possibly maghemite (e.g., Smirnov and Tarduno, 2000; Carter-Stiglitz et al., 2006; Church et al., 2011), which are both likely present in the Icelandic samples. While RTSIRM curves indicate the presence of magnetite (based on T_v), the curves also display behavior typical of oxidized (maghemitized) magnetite (based on the humped shaped cooling curve) or titanomagnetite. The amount of remanence recovered after a cooling-warming cycle ranging from 85 to 95% is not a typical true MD magnetite response. Both the FC/ZFC and RTSIRM curves more likely

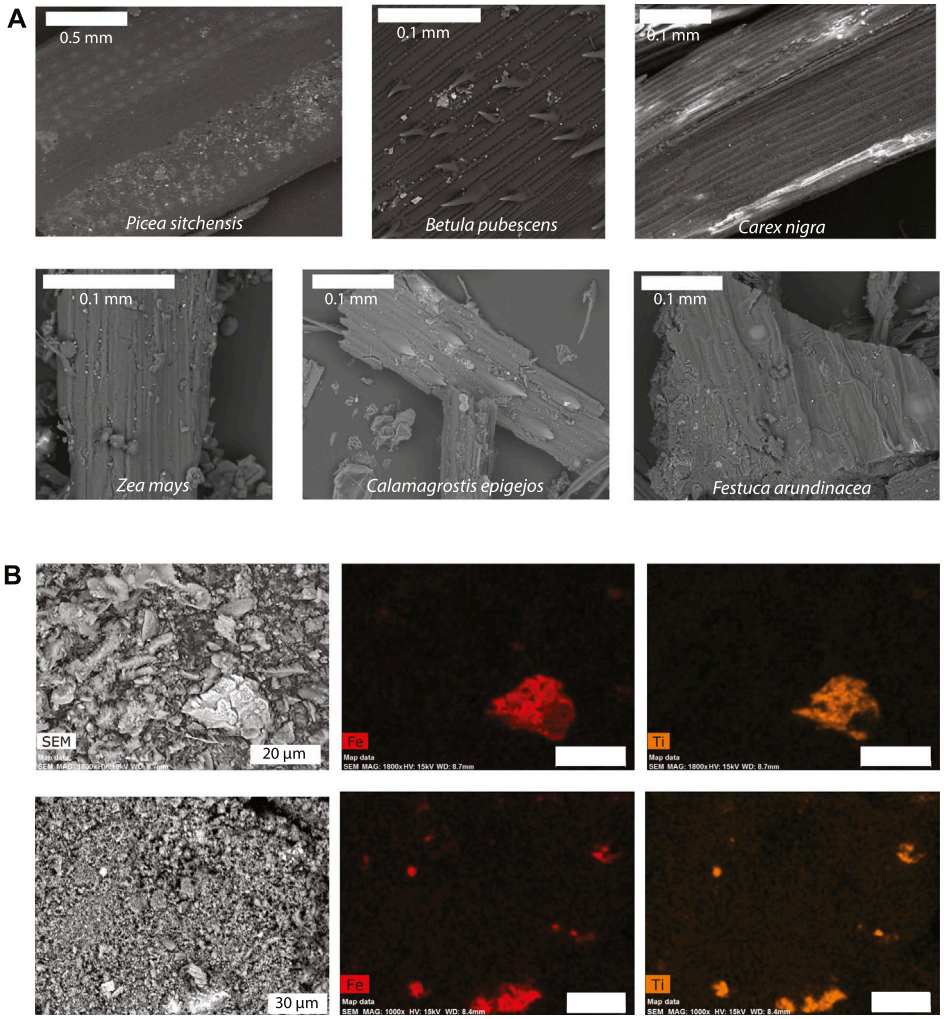

FIGURE 10 | SEM and EDS maps of plant and ash samples. **(A)** Backscattered electron images of Icelandic (top row) and German (bottom row) plant sample surfaces before burning. Small bright features are particulate matter. **(B)** EDS maps of Fe-bearing particles in Icelandic plant ash showing associations with Ti.

represent combinations of partially oxidized particles (magnetite and titanomagnetite) in the SD- to small PSD size range.

4.2 Origin of Magnetic Phases in Plant Ash

4.2.1 Inorganic Sources of Fe in Plant Ash

Plants surfaces accumulate dust through atmospheric deposition and redistribution of soil particles by wind and water, some of which may be taken up into the leaf tissue (De Nicola et al., 2008). Although cleaning treatments such as washing with water, biological detergents, weak acids, and ultrasonication are useful in reducing metal concentrations from soil and dust on the surface of plant materials (Ugolini et al., 2013), no cleaning procedure has been found to successfully remove all surface contamination (Jones and Wallace, 1992; Cook et al., 2009). This is especially true for plants with a thick waxy cuticle, in which dust and soil particles may become embedded. Residual dust and soil can produce significant overestimates of the metal content in plant tissues, especially for Fe (Jones and Wallace, 1992; Cary et al., 1994). However, the extent of soil inclusion may be estimated by determining elemental concentrations of Ti and Al, which are not present at appreciable levels in most biological materials but are abundant in soils and atmospheric dust, as well as in particulate matter from pollution sources (Cherney and Robinson, 1983; Cook et al., 2009).

An increasing number of recent studies have demonstrated that magnetic measurements of leaves, especially tree leaves in urban environments, provides a good estimate of atmospheric particulate matter (Mitchell and Maher, 2009; Hofman et al., 2014). Previous analysis of Icelandic dust by X-ray diffraction and SEM found that it is largely composed of volcanic glass, with approximately 0.7 wt% magnetite and ulvospinel (Dagsson-Waldhauserova et al., 2014). The dust and soil in Iceland are derived from basaltic parent materials and are higher in Fe, Al, and Ti than dust and soils in typical continental settings. The

strong correlation between total Fe content and M_S with Ti and Al in plant ash is likely more pronounced in Iceland than it would be in other regions. The low T_C values observed for some Icelandic samples are probably associated with titanomagnetite. Differences in soil and dust parent material composition probably account for the greater apparent enhancement in M_S after burning (without accounting for LOI) for the Icelandic plant ash compared with German plant ash.

The remaining changes in M_S with burning temperature after correcting for the loss of plant mass is attributed to thermal alteration of inorganic particulate matter. The nature of this alteration seems to vary among plant types, with significant increases in LOI-normalized M_S indicating net production of strongly magnetic minerals. This phase is presumed to be magnetite, some of which is superparamagnetic and nanosized, which is the dominant phase observed in thermomagnetic curves for ash samples (**Figure 1**). However, it is not possible to distinguish possible pyrogenic magnetite from relict lithogenic magnetite based on the available data. Decreases in saturation magnetization after burning may reflect oxidation of lithogenic Fe-oxides, as the samples were heated in air inside a muffle furnace with a large volume. However, conditions appear to have been insufficiently oxidizing during ashing to produce hematite, which was not detected in any low-temperature or thermomagnetic (in air or argon) measurements.

4.2.2 Fe in Plant Tissues

In this study we observe a clear association between saturation magnetization and Ti content (**Figure 9B**), indicating that much of the magnetic material and Fe associated with the plant material is inorganic in origin. Plant tissues contain trace amounts of Fe as a micronutrient, with typical leaf concentrations for plants grown in growth chambers in the range 10–200 ppm (Himelblau and Amasino, 2001; Garnett and Graham, 2005). In contrast, the Fe concentrations measured in our ash samples correspond to leaf concentrations ranging from 220 to over 4,000 ppm. Among various organic Fe compounds, the protein phytoferritin stores iron as a ferric hydroxide similar to ferrihydrite (Briat et al., 2015), which some studies have hypothesized may contribute to pedogenic Fe mineral assemblages in soils (Gajdardziska-Josifovska et al., 2001; McClean et al., 2001). Fe stored in ferritin and other organic compounds could potentially also transform to ferromagnetic phases during burning of live plant material. Such transformations may be partially responsible for the larger increases in M_S observed in green leaves compared to leaf litter from the same species (**Figure 7A**). However, phytoferritin and other plant proteins typically become degraded and mobilized during senescence, so ferritin is unlikely to remain intact in plant litter, which forms the bulk of the O horizon of soils. While Fe in plant tissues probably does contribute to the formation of Fe-oxide phases in plant ash, in most settings the organic component will be far outweighed by the contribution of inorganic particulate matter given the low concentrations of Fe in biological tissues compared to those in dust or soil.

4.3 Factors Influencing Magnetic Signatures of Plant Ash

Our experimental burning results indicate that the concentration of strongly magnetic phases in plant ash depends strongly on combustion temperature. The observed differences between saturation magnetization values normalized by the burnt sample mass vs. the initial plant mass demonstrate that while the concentration of magnetic material typically increases after burning at temperatures above 300°C, this increase may not necessarily reflect the formation of new magnetic phases. In many samples, most or all of the apparent increase in mass-normalized M_S can be accounted for by the loss of mass during burning.

It follows that other mass-specific magnetic properties, such as susceptibility, that appear to increase in soils following wildfire events may also dominantly reflect a reduction in organic matter mass instead of pyrogenic mineral formation or transformation. Magnetic enhancement in fire-affected soils may therefore be a reasonable proxy for organic matter loss due to burning, which supports the suggestion of Jordanova et al. (2019a) that fire intensity is directly correlated with the resulting degree of magnetic enhancement. Our results further indicate that elevated mass-specific magnetic parameters following high-intensity burning, such as forest fires, primarily occur because mass loss associated with organic matter combustion serves to increase the concentrations of inorganic magnetic particles incorporated into plant material and secondarily occur due to thermal transformation of weakly magnetic inorganic phases to strongly magnetic phases (see **Section 4.3** below).

While M_S values are consistently elevated in char and ash produced at 300 and 550°C, the extent of this increase varies substantially among plant types. This variation is likely influenced by the amount of soil and dust inclusion in plant samples surfaces, as indicated by the strong correlation of M_S with Ti content. In turn, our SEM observations indicate that Ti and particulate matter content qualitatively depend on plant type through differences in leaf texture and morphology. A study by Kardel et al. (2011) also found a species effect on leaf SIRM and the amount of retained particulate matter on urban tree leaves, where hairy or rough-textured leaves tend to accumulate more dust, while smoother, more hydrophobic leaves are more likely to shed dust. Kardel et al. (2011) additionally observed a strong seasonal affect, with particulate matter concentrations increasing throughout the growing season. Our findings also suggest that seasonality may play a role in the magnetic properties of plant ash, based on the contrasting burning-induced enhancement in green leaves compared to plant litter.

4.4 Implications for Magnetic Enhancement of Soils by Fire

Our results help to resolve seemingly conflicting results from earlier studies documenting changes in magnetic susceptibility in soils affected by fire, with some finding evidence for strong enhancement after burning (Blake et al., 2006; Clement et al., 2011, e.g.), while others find weak or no magnetic signatures of burning (Roman et al., 2013). We demonstrate that low-temperature burning even for several hours tends to decrease the magnetization of plant material, while higher burning temperatures produce significant increases in magnetization. Our finding that M_S is reduced or relatively unchanged by burning at 200°C is consistent with the observations of Roman et al. (2013), who saw no significant changes in soil magnetic properties following short-duration, moderate-intensity grass fires.

Ferric (hydr)oxides such as goethite, lepidocrocite, and ferrihydrite are common phases in dust and soil. If present on plant surfaces, these phases will easily alter on heating and can transform rapidly to magnetite and maghemite, especially in the reducing environment created by combusting organic matter (Till et al., 2017; Till and Nowaczyk, 2018). For weakly magnetic ferric phases such as goethite and hematite in soils affected by low-intensity fires, the modest rise in temperature, which is restricted to the uppermost few cm, is likely insufficient to produce thermal alteration of these minerals (Roman et al., 2013; Jordanova et al., 2019a). However, high-intensity fires can heat soil down to depths of at least 10 cm to temperatures high enough to trigger reductive alteration of goethite and hematite to magnetite or maghemite Clement et al. (2011); Nørnberg et al. (2009); Ketterings et al. (2000). Soil in Iceland, like in other volcanic regions, typically contain high concentrations of poorly crystalline phases such as ferrihydrite and allophane (up to 15 and 30%, respectively, according to Arnalds (2004)). Ferrihydrite easily alters to magnetite when heated in the presence of organic matter (Hanesch et al., 2006; Till and Nowaczyk, 2018) and is a likely source of the ferromagnetic phase detected in Icelandic plant ash samples. Pyrogenic magnetite derived from ferric (oxy)hydroxides are typically fined-grained mixtures of superparamagnetic and single-domain particles (Gendler et al., 2005; Jeleńska et al., 2010; Till et al., 2015).

Another pathway for the formation of pyrogenic magnetite is through alteration of Fe-bearing clay minerals during heating, particularly smectites. Although structural Fe in smectites is stable up to temperature of 700°C (Moskowitz and Hargraves, 1982), Hirt et al. (1993) documented the formation of magnetite from weakly adsorbed Fe on smectite surfaces after heating to more moderate temperatures above 250°C. Certain clay minerals also have the potential to partially reduce hematite to magnetite on heating above 600°C, especially in less crystalline Al-hematites (Jiang et al., 2015). The magnetic properties of fire-affected topsoils will reflect mineralogical changes created by the combustion of organic matter and incorporated surface dust, including the possible formation of pyrogenic Fe-oxides, as well as heating-induced conversion of soil minerals if soil temperatures are sufficiently high.

Ash from wildfires is often both highly mobile (Whicker et al., 2002; Pereira et al., 2015) and reactive. While magnetic enhancement of fire events may be preserved over longer timescales in sedimentary archives such as lakes and continental shelf deposits Oldfield and Crowther (2007); Kent et al. (2017), it is unclear how long fire-related magnetic enhancement may persist in soils. For example, Jordanova et al. (2019b) found that the initial enhanced magnetic signal in soils containing wildfire ash decreased over a period of 3 years, presumably due to oxidation of magnetite by weathering and biogenic processes.

Finally, in comparing our experimentally produced char and ashes with burnt plant residues created by wildfires, it is important to note that natural burning conditions are far less controlled and constant than laboratory conditions Bodí et al. (2014) and that factors such as oxygen and fuel supply as well as temperature and heat transfer Pingree and Kobziar (2019) may be highly heterogeneous in field settings. Nevertheless, laboratory burning of individual plant species is a valuable approach for distinguishing the chemistry and magnetic properties of burnt plant material from that of soils.

5 CONCLUSION

We conducted a detailed rock magnetic characterization of burnt plant residues from individual species collected in Iceland and Germany. A close correlation between total Fe and Ti in the Icelandic plant samples indicates that a significant amount of the iron in plant ash is derived from inorganic particulate matter embedded in plant surfaces, which dominates the magnetic properties of the ash. Strong increases in saturation magnetization were observed after burning at temperatures of 300°C and above, indicating increasing concentrations of ferromagnetic particles. Most of this increase is attributed to the reduction in plant mass during burning, while thermal alteration of entrained dust and soil on plant surfaces plays a lesser role in determining the magnetic properties of plant char and ash. Ash from cleaned plant material exhibited hysteresis parameters very similar to that from uncleaned plant samples but with lower saturation magnetization values, suggesting that cleaning effectively reduced the concentration of surface dust, but the main magnetic phases are the same for cleaned and uncleaned plant material. Based on our study results, we do not expect plant ash to generate a unique magnetic plant-based fingerprint of burning events. Instead, magnetic properties of vegetation ash in soil and sediments will vary with the extent of burning, time of year, the local composition of dust and soil, and plant type due to differences in leaf morphology, which strongly influences the amount of retained inorganic material.

DATA AVAILABILITY STATEMENT

The original contributions presented in the study are included in the article/**Supplementary Material**, further inquiries can be directed to the corresponding author.

AUTHOR CONTRIBUTIONS

JT conceived the study, prepared the samples, and performed magnetic measurements. BM conducted and interpreted low-temperature magnetic measurements. SP facilitated geochemical analysis and contributed to the interpretation and discussion of compositional data. All authors contributed to and approved the final manuscript.

FUNDING

This project was funded by Rannís, the Iceland Centre for Research, through a postdoctoral fellowship grant (#173743-051) to JT from the Icelandic Research Fund. Part of this work was performed as a Visiting Fellow at the Institute for Rock Magnetism (IRM) at the University of Minnesota. The IRM is a United States National Multi-user Facility supported through the Instrumentation and Facilities program of the National Science Foundation, Earth Sciences Division, and by funding from the University of Minnesota.

ACKNOWLEDGMENTS

Mike Jackson, Maxwell Brown, and Peat Solheid are thanked for support with magnetic measurements. Zena Severin is thanked for assistance with sample collection and preparation. We are grateful to Andy Hobson for laboratory assistance and support with geochemical analysis. Axel Höhn at the Leibniz Center for Landscape Agriculture (ZALF) kindly provided the German plant samples used in this study. We thank our reviewers for providing constructive comments to help improve the manuscript. This is IRM contribution 2006.

SUPPLEMENTARY MATERIAL

The Supplementary Material for this article can be found online at: https://www.frontiersin.org/articles/10.3389/feart.2020.592659/full#supplementary-material.

REFERENCES

Arnalds, O. (2004). Volcanic soils of iceland. *Catena* 56, 3–20. doi:10.1016/j.catena.2003.10.002

Bilardello, D., and Jackson, M. (2013). What do the mumpsies do? *IRM Q.* 23, 11–15.

Blake, W., Wallbrink, P., Doerr, S., Shakesby, R., and Humphreys, G. (2006). Magnetic enhancement in wildfire-affected soil and its potential for sediment-source ascription. *Earth Surf. Process. Landforms* 31, 249–264. doi:10.1002/esp.1247

Bodí, M. B., Martin, D. A., Balfour, V. N., Santín, C., Doerr, S. H., Pereira, P., et al. (2014). Wildland fire ash: production, composition and eco-hydro-geomorphic effects. *Earth Sci. Rev.* 130, 103–127. doi:10.1016/j.earscirev.2013.12.007

Briat, J. F., Dubos, C., and Gaymard, F. (2015). Iron nutrition, biomass production, and plant product quality. *Trends Plant Sci.* 20, 33–40. doi:10.1016/j.tplants.2014.07.005

Carrancho, Á., and Villalaín, J. (2011). Different mechanisms of magnetisation recorded in experimental fires: archaeomagnetic implications. *Earth Planet Sci. Lett.* 312, 176–187. doi:10.1016/j.epsl.2011.10.006

Carter-Stiglitz, B., Moskowitz, B., Solheid, P., Berquó, T. S., Jackson, M., and Kosterov, A. (2006). Low-temperature magnetic behavior of multidomain titanomagnetites: Tm0, tm16, and tm35. *J. Geophys. Res.: Solid Earth* 111, B12S05. doi:10.1029/2006JB004561

Cary, E., Grunes, D., Bohman, V., and Sanchirico, C. (1986). Titanium determination for correction of plant sample contamination by soil. *Agron. J.* 78, 933–936. doi:10.2134/agronj1986.00021962007800050038x

Cary, E., Grunes, D., Dallyn, S., Pearson, G., Peck, N., and Hulme, R. (1994). Plant Fe, Al and Cr concentrations in vegetables as influenced by soil inclusion. *J. Food Qual.* 17, 467–476. doi:10.1111/j.1745-4557.1994.tb00167.x

Cherney, J., and Robinson, D. (1983). A comparison of plant digestion methods for identifying soil contamination of plant tissue by Ti analysis. *Agron. J.* 75, 145–147. doi:10.2134/agronj1983.00021962007500010037x

Church, M., Peters, C., and Batt, C. (2007). Sourcing fire ash on archaeological sites in the Western and Northern Isles of Scotland, using mineral magnetism. *Geoarchaeology* 22, 747–774. doi:10.1002/gea.20185

Church, N., Feinberg, J. M., and Harrison, R. (2011). Low-temperature domain wall pinning in titanomagnetite: quantitative modeling of multidomain first-order reversal curve diagrams and ac susceptibility. *G-cubed* 12. doi:10.1029/2011gc003538

Clement, B. M., Javier, J., Sah, J. P., and Ross, M. S. (2011). The effects of wildfires on the magnetic properties of soils in the Everglades. *Earth Surf. Process. Landforms* 36, 460–466. doi:10.1002/esp.2060

Cook, L. L., McGonigle, T. P., and Inouye, R. S. (2009). Titanium as an indicator of residual soil on arid-land plants. *J. Environ. Qual.* 38, 188–199. doi:10.2134/jeq2007.0034

Dagsson-Waldhauserova, P., Arnalds, O., Olafsson, H., Skrabalova, L., Sigurdardóttir, G. M., Branis, M., et al. (2014). Physical properties of suspended dust during moist and low wind conditions in Iceland. *Icel. Agric. Sci.* 27, 25–39.

De Nicola, F., Maisto, G., Prati, M., and Alfani, A. (2008). Leaf accumulation of trace elements and polycyclic aromatic hydrocarbons (PAHs) in Quercus ilex L. *Environ. Pollut.* 153, 376–383. doi:10.1016/j.envpol.2007.08.008

Eiríksson, T., Björnsson, H., Gudmundsdóttir, K. B., Kristinsson, J., and Jóhannesson, T. (2010). The distribution of four trace elements (Fe, Mn, Cu, Zn) in forage and the relation to scrapie in Iceland. *Acta Vet. Scand.* 52, 34. doi:10.1186/1751-0147-52-34

Fabian, K., Shcherbakov, V. P., and McEnroe, S. A. (2013). Measuring the curie temperature. *G-cubed* 14, 947–961. doi:10.1029/2012GC004440

Gajdardziska-Josifovska, M., McCLEAN, R. G., Schofield, M. A., Sommer, C. V., et al. (2001). Discovery of nanocrystalline botanical magnetite. *Eur. J. Mineral* 13, 863–870. doi:10.1127/0935-1221/2001/0013-0863

Garnett, T. P., and Graham, R. D. (2005). Distribution and remobilization of iron and copper in wheat. *Ann. Bot.* 95, 817–826. doi:10.1093/aob/mci085

Gedye, S., Jones, R., Tinner, W., Ammann, B., and Oldfield, F. (2000). The use of mineral magnetism in the reconstruction of fire history: a case study from Lago di Origlio, Swiss Alps. *Palaeogeogr. Palaeoclimatol. Palaeoecol.* 164, 101–110. doi:10.1016/S0031-0182(00)00178-4

Gendler, T., Shcherbakov, V., Dekkers, M., Gapeev, A., Gribov, S., and McClelland, E. (2005). The lepidocrocite–maghemite–haematite reaction chain—I. Acquisition of chemical remanent magnetization by maghemite, its magnetic properties and thermal stability. *Geophys. J. Int.* 160, 815–832. doi:10.1111/j.1365-246X.2005.02550.x

Hanesch, M., Stanjek, H., and Petersen, N. (2006). Thermomagnetic measurements of soil iron minerals: the role of organic carbon. *Geophys. J. Int.* 165, 53–61. doi:10.1111/j.1365-246X.2006.02933.x

Himelblau, E., and Amasino, R. M. (2001). Nutrients mobilized from leaves of arabidopsis thaliana during leaf senescence. *J. Plant Physiol.* 158, 1317–1323. doi:10.1078/0176-1617-00608

Hirt, A., Banin, A., and Gehring, A. (1993). Thermal generation of ferromagnetic minerals from iron-enriched smectites. *Geophys. J. Int.* 115, 1161–1168. doi:10.1111/j.1365-246X.1993.tb01518.x

Hofman, J., Wuyts, K., Van Wittenberghe, S., Brackx, M., and Samson, R. (2014). Reprint of on the link between biomagnetic monitoring and leaf-deposited dust load of urban trees: relationships and spatial variability of different particle size fractions. *Environ. Pollut.* 192, 285–372. doi:10.1016/j.envpol.2014.05.006

Jackson, M., and Solheid, P. (2010). On the quantitative analysis and evaluation of magnetic hysteresis data. *G-cubed* 11, Q04Z15. doi:10.1029/2009GC002932

Jeleńska, M., Hasso-Agopsowicz, A., and Kopcewicz, B. (2010). Thermally induced transformation of magnetic minerals in soil based on rock magnetic study and

mössbauer analysis. *Phys. Earth Planet. In.* 179, 164–177. doi:10.1016/j.pepi.2009.11.004

Jiang, Z., Liu, Q., Roberts, A. P., Barrón, V., Torrent, J., and Zhang, Q. (2018). A new model for transformation of ferrihydrite to hematite in soils and sediments. *Geology* 46, 987–990. doi:10.1130/G45386.1

Jiang, Z., Liu, Q., Zhao, X., Jin, C., Liu, C., and Li, S. (2015). Thermal magnetic behaviour of al-substituted haematite mixed with clay minerals and its geological significance. *Geophys. J. Int.* 200, 130–143. doi:10.1093/gji/ggu377

Jóhannesson, T., Eiríksson, T., Gudmundsdóttir, K. B., Sigurdarson, S., and Kristinsson, J. (2007). Overview: seven trace elements in Icelandic forage. Their value in animal health and with special relation to scrapie. *Icel. Agric. Sci.* 20, 3–24.

Jones, J. B., and Wallace, A. (1992). Sample preparation and determination of iron in plant tissue samples. *J. Plant Nutr.* 15, 2085–2108. doi:10.1080/01904169209364460

Jordanova, D., Jordanova, N., Barrón, V., and Petrov, P. (2018). The signs of past wildfires encoded in the magnetic properties of forest soils. *Catena* 171, 265–279. doi:10.1016/j.catena.2018.07.030

Jordanova, N., Jordanova, D., and Barrón, V. (2019a). Wildfire severity: environmental effects revealed by soil magnetic properties. *Land Degrad. Dev.* 30, 2226–2242. doi:10.1002/ldr.3411

Jordanova, N., Jordanova, D., Henry, B., Le Goff, M., Dimov, D., and Tsacheva, T. (2006). Magnetism of cigarette ashes. *J. Magn. Magn Mater.* 301, 50–66. doi:10.1016/j.jmmm.2005.06.008

Jordanova, N., Jordanova, D., Mokreva, A., Ishlyamski, D., and Georgieva, B. (2019b). Temporal changes in magnetic signal of burnt soils–a compelling three years pilot study. *Sci. Total Environ.* 669, 729–738. doi:10.1016/j.scitotenv.2019.03.173

Kardel, F., Wuyts, K., Maher, B., Hansard, R., and Samson, R. (2011). Leaf saturation isothermal remanent magnetization (sirm) as a proxy for particulate matter monitoring: inter-species differences and in-season variation. *Atmos. Environ.* 45, 5164–5171. doi:10.1016/j.scitotenv.2019.03.173

Kent, D. V., Lanci, L., Wang, H., and Wright, J. D. (2017). Enhanced magnetization of the marlboro clay as a product of soil pyrogenesis at the paleocene–eocene boundary? *Earth Planet Sci. Lett.* 473, 303–312. doi:10.1016/j.epsl.2017.06.014

Ketterings, Q. M., Bigham, J. M., and Laperche, V. (2000). Changes in soil mineralogy and texture caused by slash-and-burn fires in Sumatra, Indonesia. *Soil Sci. Soc. Am. J.* 64, 1108–1117. doi:10.2136/sssaj2000.6431108x

Kletetschka, G., and Banerjee, S. K. (1995). Magnetic stratigraphy of Chinese loess as a record of natural fires. *Geophys. Res. Lett.* 22, 1341–1343. doi:10.1029/95GL01324

Le Borgne, E. (1960). Influence du feu sur les propriétés magnétiques du sol et sur celles du schiste et du granite. *Ann. Geophys.* 16, 159.

Lu, H., Liu, T., Gu, Z., Liu, B., Zhou, L., Han, J., et al. (2000). Effect of burning C3 and C4 plants on the magnetic susceptibility signal in soils. *Geophys. Res. Lett.* 27, 2013–2016. doi:10.1029/2000GL011459

Maher, B. A., Alekseev, A., and Alekseeva, T. (2003). Magnetic mineralogy of soils across the Russian steppe: climatic dependence of pedogenic magnetite formation. *Palaeogeogr. Palaeoclimatol. Palaeoecol.* 201, 321–341. doi:10.1016/S0031-0182(03)00618-7

McClean, R. G., and Kean, W. (1993). Contributions of wood ash magnetism to archaeomagnetic properties of fire pits and hearths. *Earth Planet Sci. Lett.* 119, 387–394. doi:10.1016/0012-821X(93)90146-Z

McClean, R. G., Schofield, M. A., Sommer, C. V., Robertson, D. P., Dick, T., Gajdardziska-Josifovska, M., et al. (2001). Botanical iron minerals correlation between nanocrystal structure and modes of biological self-assembly. *Eur. J. Mineral.* 13, 1235–1242. doi:10.1127/0935-1221/2001/0013-1235

Mitchell, R., and Maher, B. A. (2009). Evaluation and application of biomagnetic monitoring of traffic-derived particulate pollution. *Atmos. Environ.* 43, 2095–2103. doi:10.1016/j.atmosenv.2009.01.042

Moskowitz, B. M., and Hargraves, R. B. (1982). Magnetic changes accompanying the thermal decomposition of nontronite (in air) and its relevance to martian mineralogy. *J. Geophys. Res.: Solid Earth.* 87, 10115–10128. doi:10.1029/JB087iB12p10115

Nørnberg, P., Vendelboe, A. L., Gunnlaugsson, H. P., Merrison, J. P., Finster, K., and Jensen, S. K. (2009). Comparison of the mineralogical effects of an experimental forest fire on a goethite/ferrihydrite soil with a topsoil that contains hematite, maghemite and goethite. *Clay Miner.* 44, 239–247. doi:10.1180/claymin.2009.044.2.239

Oldfield, F., and Crowther, J. (2007). Establishing fire incidence in temperate soils using magnetic measurements. *Palaeogeogr. Palaeoclimatol. Palaeoecol.* 249, 362–369. doi:10.1016/j.palaeo.2007.02.007

Özdemir, Ö., and Dunlop, D. J. (2010). Hallmarks of maghemitization in low-temperature remanence cycling of partially oxidized magnetite nanoparticles. *J. Geophys. Res.: Solid Earth.* 115, B02101. doi:10.1029/2009JB006756

Pereira, P., Cerdà, A., Úbeda, X., Mataix-Solera, J., Arcenegui, V., and Zavala, L. (2015). Modelling the impacts of wildfire on ash thickness in a short-term period. *Land Degrad. Dev.* 26, 180–192. doi:10.1002/ldr.2195

Peters, C., and Batt, C. (2002). Dating and sourcing fuel ash residues from Cladh Hallan, South Uist, Scotland, using magnetic techniques. *Phys. Chem. Earth, Parts A/B/C.* 27, 1349–1353. doi:10.1016/S1474-7065(02)00132-8

Peters, C., Church, M., and Mitchell, C. (2001). Investigation of fire ash residues using mineral magnetism. *Archaeol. Prospect.* 8, 227–237. doi:10.1002/arp.171

Petrovskỳ, E., and Kapička, A. (2006). On determination of the curie point from thermomagnetic curves. *J. Geophys. Res.: Solid Earth* 111, B12S27. doi:10.1029/2006JB004507

Petrovskỳ, E., Remeš, J., Kapička, A., Podrázskỳ, V., Grison, H., and Borůvka, L. (2018). Magnetic mapping of distribution of wood ash used for fertilization of forest soil. *Sci. Total Environ.* 626, 228–234. doi:10.1016/j.scitotenv.2018.01.095

Pingree, M. R., and Kobziar, L. N. (2019). The myth of the biological threshold: a review of biological responses to soil heating associated with wildland fire. *For. Ecol. Manag.* 432, 1022–1029. doi:10.1016/j.foreco.2018.10.032

Roman, S. A., Johnson, W. C., and Geiss, C. E. (2013). Grass fires—an unlikely process to explain the magnetic properties of prairie soils. *Geophys. J. Int.* 195, 1566–1575. doi:10.1093/gji/ggt349

Smirnov, A. V., and Tarduno, J. A. (2000). Low-temperature magnetic properties of pelagic sediments (ocean drilling program site 805c): tracers of maghemitization and magnetic mineral reduction. *J. Geophys. Res.: Solid Earth* 105, 16457–16471. doi:10.1029/2000JB900140

Till, J. L., and Nowaczyk, N. (2018). Authigenic magnetite formation from goethite and hematite and chemical remanent magnetization acquisition. *Geophys. J. Int.* 213, 1818–1831. doi:10.1093/gji/ggy083

Till, J., Guyodo, Y., Lagroix, F., Morin, G., and Ona-Nguema, G. (2015). Goethite as a potential source of magnetic nanoparticles in sediments. *Geology* 43, 75–78. doi:10.1130/G36186.1

Till, J., Guyodo, Y., Lagroix, F., Ona-Nguema, G., and Brest, J. (2014). Magnetic comparison of abiogenic and biogenic alteration products of lepidocrocite. *Earth Planet Sci. Lett.* 395, 149–158. doi:10.1016/j.epsl.2014.03.051

Till, J. L., Guyodo, Y., Lagroix, F., Morin, G., Menguy, N., and Ona-Nguema, G. (2017). Presumed magnetic biosignatures observed in magnetite derived from abiotic reductive alteration of nanogoethite. *Compt. Rendus Geosci.* 349, 63–70. doi:10.1016/j.crte.2017.02.001

Ugolini, F., Tognetti, R., Raschi, A., and Bacci, L. (2013). Quercus ilex L. as bioaccumulator for heavy metals in urban areas: effectiveness of leaf washing with distilled water and considerations on the trees distance from traffic. *Urban For. Urban Green.* 12, 576–584. doi:10.1016/j.ufug.2013.05.007

Vassilev, S. V., Baxter, D., Andersen, L. K., and Vassileva, C. G. (2010). An overview of the chemical composition of biomass. *Fuel* 89, 913–933. doi:10.1016/j.fuel.2009.10.022

Wang, D., and Van der Voo, R. (2004). The hysteresis properties of multidomain magnetite and titanomagnetite/titanomaghemite in mid-ocean ridge basalts. *Earth Planet Sci. Lett.* 220, 175–184. doi:10.1016/S0012-821X(04)00052-4

Whicker, J. J., Breshears, D. D., Wasiolek, P. T., Kirchner, T. B., Tavani, R. A., Schoep, D. A., et al. (2002). Temporal and spatial variation of episodic wind erosion in unburned and burned semiarid shrubland. *J. Environ. Qual.* 31, 599–612. doi:10.2134/jeq2002.5990

Xiong, Y., Guilbaud, R., Peacock, C. L., Cox, R. P., Canfield, D. E., Krom, M. D., et al. (2019). Phosphorus cycling in Lake Cadagno, Switzerland: a low sulfate euxinic ocean analogue. *Geochem. Cosmochim. Acta* 251, 116–135. doi:10.1016/j.gca.2019.02.011

Conflict of Interest: The authors declare that the research was conducted in the absence of any commercial or financial relationships that could be construed as a potential conflict of interest.

The reviewer NJ declared a past co-authorship with one of the authors JT to the handling editor.